Visualizing mechanical tension across membrane receptors with a fluorescent sensor

Daniel R Stabley, Carol Jurchenko, Stephen S Marshall & Khalid S Salaita

We report a fluorescence-based turn-on sensor for mapping the mechanical strain exerted by specific cell-surface proteins in living cells. The sensor generates force maps with high spatial and temporal resolution using conventional fluorescence microscopy. We demonstrate the approach by mapping mechanical forces during the early stages of regulatory endocytosis of the ligand-activated epidermal growth factor receptor (EGFR).

The interplay between physical inputs and chemical reaction cascades coordinates a diverse set of biological processes that range from epithelial cell adhesion and migration to stem cell differentiation and immune response[1,2]. The majority of these mechanical inputs are sensed and transduced through membrane receptors that mount a signaling cascade depending on the mechanical properties of their specific cognate ligands[2]. A major challenge to understanding the molecular mechanisms of mechanotransduction is in the development of tools that can be used to measure forces applied to specific receptors on the cell surface[3].

To address this challenge, two main classes of techniques have been developed. The first class uses single-molecule force spectroscopy methods such as atomic force microscopy and optical or magnetic tweezers to measure forces at specific sites on the cell surface[3,4]. These approaches provide key measurements for cell-surface receptors, but the inherent serial nature of single-molecule force spectroscopy methods coupled with the need for statistically significant datasets in cell biology has hampered their widespread adoption[4]. The second category of approaches developed for measuring biophysical forces *in vivo* is the genetically encoded protein-tension sensors[5–7]. These sensors are composed of three domains that include a pair of fluorescent proteins linked via an elastic amino-acid domain and inserted into a suitable site in a host protein. However, the vast majority of membrane proteins and many structurally sensitive cytoplasmic proteins will not regain wild-type function upon splitting and insertion of the tension sensor into the host protein. In the absence of methods for measuring mechanical tension across the hundreds or thousands of proteins on the cell membrane or structurally sensitive soluble proteins, understanding chemo-mechanical couplings will remain a considerable challenge.

Here we report a molecular-tension sensor that can be used to spatially and temporally map forces exerted by cell-surface receptors. The sensor consists of a flexible linker that is covalently conjugated to a biological ligand at one terminus and anchored onto a surface (via a biotin-streptavidin interaction) such that mechanical forces do not result in sensor translocation (**Fig. 1a**,**b**). We chose a linker comprised of a polyethylene glycol (PEG) polymer because of its unique properties that include: (i) well-characterized and reversible force-extension curves[8,9], (ii) biocompatibility[10] and (iii) minimal nonspecific interactions with other biomolecules[11]. We functionalized the ligand and the surface with fluorophore and quencher molecules, respectively. Cellular forces exerted on the ligand extend the linker from its relaxed conformational state and remove the fluorophore from proximity to the quencher, thus resulting in increased fluorescence intensity and providing a signal to map mechanical tension transduced through specific receptor targets (**Fig. 1b** and **Supplementary Video 1**). The approach is, in principle, noninvasive and can be used to map forces with single-molecule spatial resolution and high temporal resolution in living cells. Notably, this method only requires the use of a conventional fluorescence microscope and precludes the necessity of genetic engineering of target receptors.

As a proof of concept, we used our tension sensor to map forces associated with initial uptake and trafficking of the epidermal growth factor receptor (EGFR) upon binding to its cognate ligand. The EGFR pathway has important roles in cell survival, proliferation and differentiation, and internalization is an important regulatory component in the normal physiology of this pathway[12]; it is one of the most widely studied experimental systems for investigating ligand-induced receptor endocytosis. Still, fundamental questions about the role and even the existence of forces in shuttling the receptor from the cell membrane to endosomal compartments remain[3]. It seems rational to conclude that the process of endocytosis requires the application of a force to transport the EGFR-EGF complex, but specific evidence is thus far lacking[13].

We synthesized tension sensors that present the EGF ligand and can be used to specifically measure force transmission through the EGFR (**Fig. 1** and **Supplementary Fig. 1**). To characterize the conformation of the sensor in the resting state (in the absence of cellular forces), we tethered the EGF-PEG conjugate to a fluid supported lipid bilayer. The supported lipid bilayer surface provides a well-controlled biomimetic environment in which the protein density can be quantitatively measured and tuned[14]. The sensors are homogeneously displayed on the laterally mobile supported

Department of Chemistry, Emory University, Atlanta, Georgia, USA. Correspondence should be addressed to K.S.S. (k.salaita@emory.edu).

RECEIVED 13 MAY; ACCEPTED 27 SEPTEMBER; PUBLISHED ONLINE 30 OCTOBER 2011; DOI:10.1038/NMETH.1747

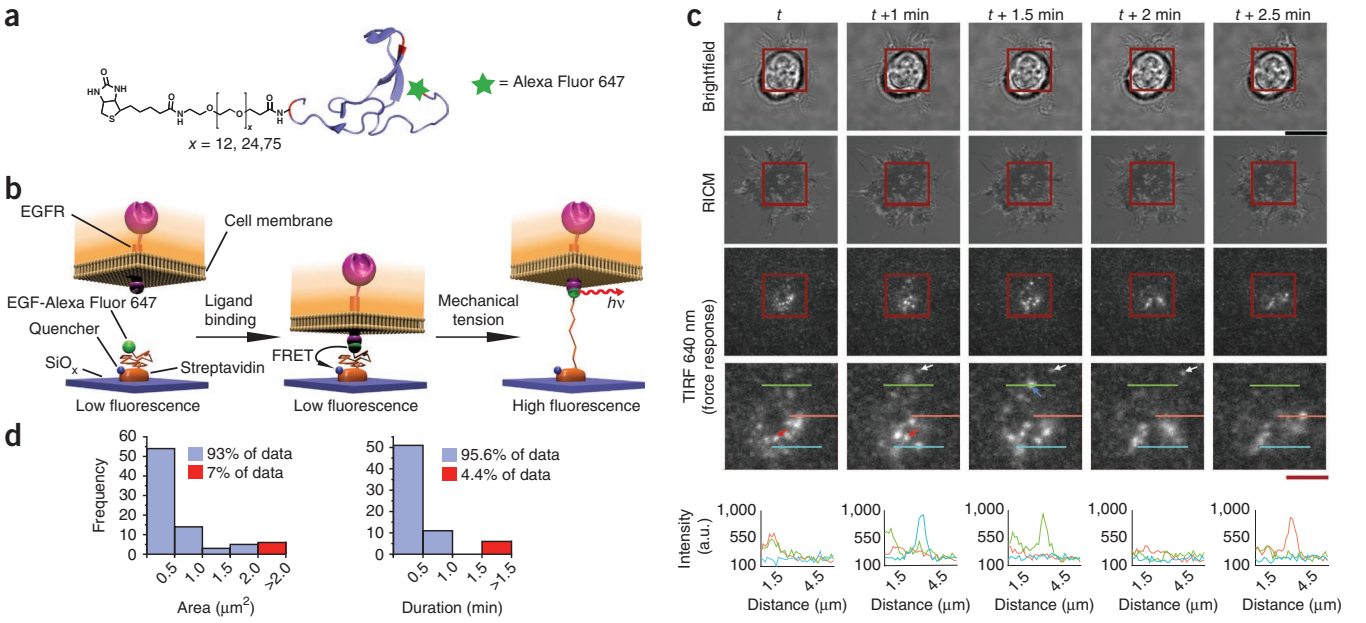

Figure 1 | Design and response of the EGFR tension sensor. (**a**) Schematic of the EGF-PEG$_x$ (x = 12, 24 or 75) tension sensor, comprised of a PEG polymer of length x that is flanked by fluorescently labeled (Alexa Fluor 647) EGF ligand and a biotin moiety for surface immobilization via streptavidin capture. EGF crystal structure adapted from Protein Data Bank (identifier IJL9). Residues in red in the crystal structure represent lysine and the N terminus, which are the available sites for PEG and fluorophore modification. (**b**) Schematic of the mechanism of sensor function. When EGFR exerts a force on its ligand, the flexible PEG linker extends. The displacement of the EGF ligand results in an increase in the measured fluorescence intensity, thus reporting the transmission of mechanical tension through the EGF-EGFR complex. $h\nu$, emission of a photon. (**c**) Representative brightfield, reflection interference contrast microscopy (RICM) and EGFR tension sensor TIRF response of HCC1143 cells plated onto sensor surfaces at 37 °C for the indicated time points (t represents the start of imaging). Images on the bottom show magnification of the boxed regions. Colored line scans represent 34 pixel profiles through the indicated region; the color of each line corresponds to the graph shown below each set of frames. The white, red and blue arrows highlight fluorescent spots that persisted for 90 s, 60 s and 30 s, respectively. Black scale bar, 20 μm; red scale bar, 4 μm. Fluorescence intensity is given in arbitrary units (a.u.). (**d**) Histograms of the areas (n = 82) and the durations (n = 68) of fluorescent points under a cell that was observed for 10 min.

lipid bilayer surface as indicated by fluorescence recovery after photobleaching (**Supplementary Fig. 2**). Quantitative fluorescence resonance energy transfer (FRET) efficiency measurements showed that the sensor conjugates adopted a condensed mushroom-like conformation with the EGF located 5.5 ± 0.1 nm, 5.2 ± 0.2 nm and 7.0 ± 0.2 nm (mean ± s.e.m., n = 3) from the surface for the EGF-PEG$_x$ conjugates, where x = 12, 24 and 75 monomer units, respectively (**Supplementary Fig. 2**). These distance values suggest that the EGF-PEG$_{24}$ and EGF-PEG$_{75}$ linkers adopt their predicted Flory radii[8,9,15]. Consequently, the resting-state structures of the EGF-PEG$_{75}$ and EGF-PEG$_{24}$ sensor conjugates were at ~25% and ~57% of their full contour lengths, respectively, which implies that the fluorescence intensity is expected to increase considerably as the PEG linkers are fully extended. Although the conformation of PEG polymers in solution is temperature- and solvent-dependent[8,15], we found that the equilibrium conformation of the force sensor was not appreciably altered at physiological conditions (37 °C and 1× phosphate-buffered saline (pH 7.4)) (**Supplementary Fig. 3**). Therefore, these data, along with experimental and theoretical literature precedent investigating the force extension of PEG polymers and their protein conjugates[8,9,16,17], predict that the dynamic range of the EGF-PEG force sensors directly depends on the length of the PEG linker. For example, the dynamic range of EGF-PEG$_{24}$ conjugates is expected to be 0–20 pN, and >95% of the maximum fluorescence intensity will be observed with the application of a 20 pN force (**Supplementary Fig. 4**). This range is compatible with the range of forces inherent to many biological processes[1,3,5].

When we engaged immortalized human breast cancer cells (HCC1143) to the EGFR tension sensor surface, receptors expressed in the cell membrane bound to their cognate ligands. Within 20–30 min of cell spreading, we observed transient and localized increases in fluorescence intensity via time-lapse total internal reflection fluorescence (TIRF) microscopy, which exclusively probes molecules within 150 nm of the substrate (**Fig. 1c** and **Supplementary Video 2**). The bright spots were diffraction-limited (**Fig. 1c**,**d**), suggesting that the observed events were localized to punctate points that experience mechanical tension. Additional analysis revealed that the localized increases in fluorescence were short-lived, seldom persisting longer than 30 s, and that there was a range of lifetime distributions for points across the cell-substrate contact plane (**Fig. 1c**,**d**). The fluorescence intensity at these spots then returned to the background amount, indicating that the fluorophore-labeled EGF remains bound to the sensor surface. We did not observe noteworthy photobleaching under these time-lapse imaging conditions during the first 20–30 frames. The recovery of the fluorescence intensity to the background level after the transient increase may be a consequence of ligand-receptor dissociation or diminished cellular pulling, and we could not distinguish between these two events in these experiments. The mechanism of complete internalization is most likely stalled because the ligand is tethered to the substrate, and thus the measured mechanical forces are associated with the initial steps of ligand uptake.

Given that a wide array of adhesion receptors may interact with the underlying substrate, we tested the specificity of our tension

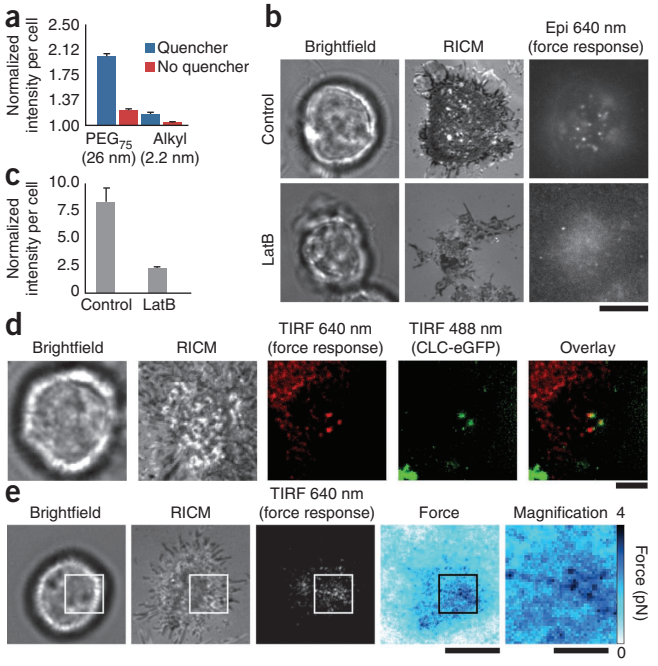

Figure 2 | Characterization and quantification of the EGFR tension sensor. (**a**) Role of the flexible linker (alkyl, 2.2 nm or PEG_{75}, 26 nm) and the quencher in the EGFR tension sensor response. Error bars, s.e.m. (n = 77 cells). (**b**) Representative brightfield, reflection interference contrast microscopy (RICM) and EGFR tension sensor response (epifluorescence (epi) 640 nm) channels for cells treated with latrunculin B (LatB) or control (DMSO). Scale bar, 5 µm. (**c**) Measured EGF force response (normalized fluorescence intensity) between LatB-treated (n = 33 cells) and untreated (n = 32 cells). Error bars, s.e.m. (**d**) Representative dual channel TIRF microscopy images of a *CLC-eGFP*–transfected cell engaged to the force-sensing surface. Overlay channel shows colocalization of CLC-eGFP and the EGF-force response. Scale bar, 5 µm. (**e**) Representative brightfield, RICM and fluorescence response for a cell engaged to an EGF-PEG_{24} force sensor surface. The sensor fluorescence response was converted into a force map by using the extended WLC model for PEG_{24}. Scale bars, 10 µm (3.2 µm in the magnified image).

sensor to EGFR using three sets of control experiments. First, we synthesized bovine serum albumin (BSA) force-sensor conjugates and plated cells on these substrates. The BSA conjugates under the cells displayed no fluorescence response as detected by TIRF imaging 30 min after plating (**Supplementary Fig. 5**). Second, we pretreated cells with 1.7 nM soluble EGF for 5 min, then plated these cells on the EGF force-sensor surfaces and also did not observe an optical response (**Supplementary Fig. 6**). Finally, to determine the role of an apposed ligand in the specificity of the force response, we incorporated a cyclic Arg-Gly-Asp (RGD) peptide ligand into the BSA-force sensor surface. Unlike the first two controls, cells strongly engaged these surfaces, as indicated by reflection interference contrast microscopy imaging, but the observed fluorescence response was negligible (**Supplementary Fig. 7**). Taken together, these experiments confirmed that the measured responses were specific to force transmission through the EGFR.

To examine the role of the PEG linker and the specific fluorophore (Alexa Fluor 647) and quencher (QSY 21) pair (Förster radius, R_0 = 6.9 nm according to the manufacturer) in the observed fluorescence response, we performed cell-tension measurements with sensors displaying short linkers (contour length of 2.2 nm) or with sensors that lacked the quencher tags. In these experiments, we quantified the force response in single cells and normalized it to the background signal (**Supplementary Fig. 8**). Experiments with sensors containing a 2.2-nm linker showed minimal response when compared to the 26-nm PEG_{75} linkers (**Fig. 2a**). Similarly, sensors that lacked the quencher did not exhibit a notable fluorescence increase (**Fig. 2a** and **Supplementary Fig. 9**). To eliminate the possibility that direct ligand-receptor binding may lead to sensor response, we treated EGF force-probe surfaces with a monoclonal EGF antibody. This treatment did not result in a sensor response (**Supplementary Fig. 10**). To ensure that the biological activity of the EGF ligand was not influenced by the length (flexibility) of the different linkers, we immunostained cells with an antibody to phospho (p)Tyr1068 of EGFR to measure the relative activation. Single-cell fluorescence analysis did not indicate a marked difference in immunostaining between cells activated with tension-sensor surfaces that used 2.2-nm or 26-nm linker contour lengths, thus showing that cells were similarly activated (**Supplementary Fig. 11**). Overall, these experiments showed that the tension sensor requires a flexible linker that is appropriately matched to the Förster radius of the dye pair.

EGFR endocytosis is thought to primarily proceed through an internalization pathway that is mediated through the cytoskeleton and clathrin-coated pits[12]. To look for evidence for the role of the cytoskeleton in mechanotransduction, we treated cells with latrunculin B, a cytoskeletal inhibitor that targets the assembly of F-actin. This led to a 70% reduction in sensor response, indicating that physical tension is dependent on proper function of the cytoskeleton (**Fig. 2b**,**c**). To confirm that mechanical force is associated with clathrin-coated pit invagination, we transiently transfected the HCC1143 cells with a construct encoding clathrin light chain–enhanced GFP (eGFP) (*CLC-eGFP*). Using live-cell dual-channel TIRF microscopy we measured the association of CLC-eGFP with the EGFR tension sensor. We observed diffraction-limited bright spots in both fluorescence channels (**Fig. 2d** and **Supplementary Video 3**). Taken together, the average lifetimes and dimensions of the punctate points along with actin-dependence and clathrin-colocalization data all confirm that the mechanical pulling events are consistent with a clathrin-mediated EGF internalization mechanism[18].

Our tension sensor design allows for precise quantification of the magnitude of the applied force required to extend the PEG linker from its resting state. We determined the physical extension of the linker from the FRET relation and then used this displacement to estimate the mechanical tension using the extended worm-like chain (WLC) model (Online Methods)[8,9,16]. This conversion is possible owing to the fact that PEG is a well-behaved polymer whose force-extension profile experimentally fits the extended WLC with high accuracy (less than 1% error) in 1× PBS buffer[16] (**Supplementary Fig. 12**). We used monolabeled EGF-PEG_{24} conjugates because of their broad dynamic range for force quantification. We generated a representative force map for a cell that engaged the EGF tension sensor for 30 min (**Fig. 2e**). The punctate fluorescent regions showed a peak force value of approximately 4 pN, which represents the lower-bound ensemble average force applied by the EGF receptor on that area.

Our tension sensor design provides a general method for mapping mechanical tension experienced by specific membrane proteins on the surface of living cells. These tension maps provide, to our knowledge, the first direct evidence showing that mechanical forces are associated with the initial stages of EGF ligand internalization. This method could be applied to rapidly study chemomechanical interactions across nearly any receptor or cell type. The inherent flexibility of the platform may also enable the investigation of mechanical force transmission across cell-cell junctions, such as those between T cells and antigen-presenting cells as well as epithelial cell junctions, which are typically not amenable to direct investigations by other methods.

METHODS

Methods and any associated references are available in the online version of the paper at http://www.nature.com/naturemethods/.

Note: Supplementary information is available on the Nature Methods website.

ACKNOWLEDGMENTS

We thank A. Mattheyses (Emory University) for the *CLC-eGFP* plasmid and R. Nahta (Emory University Winship Cancer Institute) for the HCC1143 cells. We acknowledge the Emory University Winship Cancer Institute for support. K.S.S. acknowledges the Georgia Cancer Coalition Cancer Research Award for its support.

AUTHOR CONTRIBUTIONS

D.R.S. adapted the FRET surface sensor for use with human cells expressing the EGFR and performed the majority of the human cell experiments. C.J. developed the force sensor and performed the quantitative characterization of the zero-force sensor conformation and its components. S.S.M. optimized and performed the *CLC-eGFP* transfections. K.S.S. devised the overall experimental strategy. D.R.S., C.J. and K.S.S. wrote and edited the manuscript.

COMPETING FINANCIAL INTERESTS

The authors declare no competing financial interests.

Published online at http://www.nature.com/naturemethods/.
Reprints and permissions information is available online at http://www.nature.com/reprints/index.html.

1. Vogel, V. & Sheetz, M. *Nat. Rev. Mol. Cell Biol.* **7**, 265–275 (2006).
2. DuFort, C.C., Paszek, M.J. & Weaver, V.M. *Nat. Rev. Mol. Cell Biol.* **12**, 308–319 (2011).
3. Dufrene, Y.F. *et al. Nat. Methods* **8**, 123–127 (2011).
4. Muller, D.J., Helenius, J., Alsteens, D. & Dufrene, Y.F. *Nat. Chem. Biol.* **5**, 383–390 (2009).
5. Grashoff, C. *et al. Nature* **466**, 263–266 (2010).
6. Iwai, S. & Uyeda, T.Q.P. *Proc. Natl. Acad. Sci. USA* **105**, 16882–16887 (2008).
7. Meng, F. & Sachs, F. *J. Cell Sci.* **124**, 261–269 (2011).
8. Oesterhelt, F., Rief, M. & Gaub, H.E. *New J. Phys.* **1**, 6.1–6.11 (1999).
9. Kienberger, F. *et al. Single Molecules* **1**, 123–128 (2000).
10. Roberts, M.J., Bentley, M.D. & Harris, J.M. *Adv. Drug Deliv. Rev.* **54**, 459–476 (2002).
11. Harder, P., Grunze, M., Dahint, R., Whitesides, G.M. & Laibinis, P.E. *J. Phys. Chem. B* **102**, 426–436 (1998).
12. Goh, L.K., Huang, F., Kim, W., Gygi, S. & Sorkin, A. *J. Cell Biol.* **189**, 871–883 (2010).
13. Martin, A.C., Welch, M.D. & Drubin, D.G. *Nat. Cell Biol.* **8**, 826–833 (2006).
14. Salaita, K. *et al. Science* **327**, 1380–1385 (2010).
15. de Gennes, P.G. *Macromolecules* **13**, 1069–1075 (1980).
16. Bouchiat, C. *et al. Biophys. J.* **76**, 409–413 (1999).
17. Sulchek, T.A. *et al. Proc. Natl. Acad. Sci. USA* **102**, 16638–16643 (2005).
18. Saffarian, S., Cocucci, E. & Kirchhausen, T. *PLoS Biol.* **7**, e1000191 (2009).

ONLINE METHODS

Synthesis and characterization of streptavidin-quencher conjugates. A streptavidin labeling ratio of 1 was desired to accurately use the FRET relation and determine the zero-force conformation of the sensor. Recombinant streptavidin (Rockland Immunochemicals) was labeled with quencher by mixing 300 µg of the protein in 150 µl of 1× PBS (10 mM phosphate buffer, 137 mM NaCl, pH 7.4) with 15 µl of 1 M sodium bicarbonate and a 20-fold molar excess of QSY 21 *N*-hydroxysuccinimide (NHS) ester (Invitrogen). The reaction was allowed to proceed for 60 min at room temperature (23 °C) on a rotating platform. Purification was performed by size-exclusion chromatography using Bio-Gel P4 resin (Bio-Rad) swollen with 1× PBS. The final product was characterized using matrix-assisted laser desorption–time-of-flight (MALDI-TOF) and absorbance spectrometry. The labeling ratio was determined to be 0.8 by UV-visible light absorbance measurements of the gel-purified product.

For all other experiments, recombinant streptavidin was labeled with quencher by mixing 1 mg ml^{-1} of the protein in 1× PBS with an excess of QSY 21 NHS ester. The reaction was allowed to proceed for 60 min at room temperature, and the tube was inverted every 15 min to ensure proper mixing. The product was purified with a Slide-a-Lyzer Mini dialysis column (Thermo Fisher) with a cutoff of 3,500 g mol^{-1} following manufacturer recommendations and performing a 30 min dialysis in a 2-l bath of 1× PBS twice. The final product was characterized using MALDI-TOF and absorbance spectrometry. Empirically, we found that a five-fold molar excess of QSY 21 achieved a labeling ratio of ~0.9–1.1. In contrast, a 20-fold molar excess of QSY 21 yielded streptavidin with a labeling ratio of ~2 when using this method, based on UV-visible light absorbance measurements.

Synthesis and characterization of EGF-PEG conjugates. EGF was simultaneously labeled with a flexible biotinylated PEG linker (PEG_{12} (Thermo Scientific), PEG_{24} (Quanta Biodesign) or PEG_{75} (Nanocs)) and fluorescent dye (Alexa Fluor 647 (Invitrogen)) in a single pot reaction using standard NHS bioconjugation chemistry. A monolabeled product for both PEG and dye was desired for quantitative experiments. The optimal reaction concentrations were empirically determined to be 120 µM EGF, 0.1 M sodium bicarbonate and a fivefold molar excess of both the biotin-PEG NHS ester and the Alexa Fluor 647 NHS ester. The reaction was incubated on a rotating platform at room temperature for 30 min and purified using the Bio-Gel P6 resin (Bio-Rad). MALDI-TOF mass spectrometry and UV-visible light absorbance measurements were used to determine the overall EGF:PEG:dye ratio (data not shown). Mass spectrometry indicated that the predominant product under these reaction conditions had an EGF:PEG:dye ratio of 1:1:1. Note that other EGF:PEG:dye stoichiometries existed in the sample, the most abundant of which was dual labeled with dye but not conjugated to the biotin-PEG anchor (1:0:2) and therefore would not adhere to the streptavidin-functionalized surfaces.

In some cases, EGF was labeled with biotinylated PEG_{75} and Alexa Fluor 647 in a step-wise fashion. First, 10 µl of 1 M sodium bicarbonate was added to 100 µl of EGF (1 mg ml^{-1}), then 20-fold molar excess of Alexa Fluor 647 NHS ester was added and the reaction was allowed to proceed for 10 min at room temperature. Subsequently, a 15-fold molar excess of biotin-PEG_{75} NHS ester was added to the reaction mixture and allowed to incubate for an additional 30 min. The reaction was purified using Bio-Gel P6 resin (Bio-Rad). The final labeling ratio of dye:protein, as measured by UV-visible light absorbance, was 0.8. The EGF that was used for the alkyl linker controls was labeled in a single-pot reaction with NHS-sulfo-LC-biotin (LC, long chain) (Pierce) and Alexa Fluor 647 NHS ester (Invitrogen). We added 20 µl of 1 M sodium bicarbonate to 200 µl of 1 mg ml^{-1} EGF, after which a 20-fold molar excess of both biotinylated linker and dye was added. After reagent addition, the reaction was incubated for 1 h at room temperature and inverted every 15 min to ensure mixing. The reaction mixture was subsequently purified with Bio-Gel P4 resin (Bio-Rad), yielding EGF with an Alexa Fluor 647 labeling ratio of 1.9.

Cell culture. HCC1143 cells were cultured in RPMI 1640 medium (Mediatech) supplemented with 10% FBS (Mediatech), HEPES (9.9 mM, Sigma), sodium pyruvate (1 mM, Sigma), L-glutamine (2.1 mM, Mediatech), penicillin G (100 IU ml^{-1}, Mediatech) and streptomycin (100 µg ml^{-1}, Mediatech) and were incubated at 37 °C with 5% CO_2. Cells were passaged at 90–100% confluency and plated at a density of 50% using standard cell culture procedures. All experiments were conducted with HCC1143 cells that had been serum-starved for ~18 h.

Functionalization of glass substrate biosensors. Glass coverslips were functionalized based on literature precedent[19]. Briefly, glass coverslips (number 2, 25-mm diameter; VWR) were sonicated in Nanopure water (18.2 mΩ) for 10 min and then etched in piranha (a 3:1 mixture of sulfuric acid (Avantor Performance Materials) and hydrogen peroxide (Sigma)) for 10 min (please take caution: piranha is extremely corrosive and may explode if exposed to organics). The glass coverslips were then washed six times in a beaker of Nanopure water (18.2 mΩ) and placed into three successive wash beakers containing EtOH (Decon Labs) and left in a final fourth beaker containing 1% (3-aminopropyl)triethoxysilane (APTES, Sigma) in EtOH for 1 h. The substrates were then immersed in the EtOH three times and subsequently rinsed with EtOH and dried under nitrogen. Substrates were then baked in an oven (~100 °C) for 10 min. After cooling, the samples were incubated with NHS-biotin (Thermo Fisher) at 2 mg ml^{-1} in DMSO (Sigma) overnight. Subsequently, the substrates were washed with EtOH and dried under nitrogen. The substrates were then washed with 1× PBS (3 × 5 ml aliquots) and incubated with BSA (EMD Chemicals, 100 µg $µl^{-1}$, 30 min) and washed again with 1× PBS (3 × 5 ml aliquots). Quench labeled streptavidin was then added (1 µg ml^{-1}, 45 min, room temperature) followed by washing with 1× PBS (3 × 5 ml aliquots) and incubating with the desired EGF construct (biotinylated linker and fluorophore labeled, 1 µg ml^{-1}, 45 min, room temperature). Substrates were then rinsed with a final wash of 1× PBS (3 × 5 ml aliquots) and used within the same day. To verify that surfaces were stable within the experimental time frame, a substrate, functionalized as described above, was imaged over two consecutive days. The fluorescence intensity of the surface did not change greatly within this time frame (**Supplementary Fig. 13**).

Functionalization of supported lipid bilayers. Lipids consisted of 99.9% 1,2-dioleoyl-*sn*-glycero-3-phosphocholine (DOPC, Avanti Polar Lipids) and 0.1% 1,2-dioleoyl-*sn*-glycero-3-phosphoethanolamine-N-(cap biotinyl) (sodium salt) (DPPE-biotin, Avanti Polar Lipids). After being mixed in the correct proportions

in chloroform, lipids were dried with a rotary evaporator and placed under a stream of N_2 to ensure complete evaporation of the solvent. These lipid samples were then resuspended in Nanopure water and subjected to three freeze-thaw cycles by alternating immersions in an acetone and dry ice bath and a warm water bath (40 °C). To obtain small unilamellar vesicle, lipids were extruded through a high-pressure extruder with a 100-nm nanopore membrane (Whatman)[20].

Supported lipid bilayers were assembled by adding small unilamellar vesicles to base-etched 96-well plates with glass-bottomed wells. At the biotinylated lipid doping concentration used (0.1%), the calculated streptavidin density was 690 molecules μm^{-2}, and therefore it is expected that streptavidin bound to the surface was at sufficiently low density to avoid fluorophore self-quenching[21]. This was confirmed by measuring fluorescence intensity as a function of biotin doping concentration (data not shown). After blocking with BSA (0.1 mg ml^{-1}) for 30 min, bilayer surfaces were incubated with either unlabeled streptavidin (1 µg 400 μl^{-1}) or streptavidin QSY 21 (1 µg 400 μl^{-1}) for 1 h. Wells were rinsed 3× with 5 ml of 1× PBS, then incubated with EGF-PEG_x–Alexa Fluor 647 (100 nM) (x = 12, 24 or 75) for 1 h and rinsed 3× with 5 ml of 1× PBS before imaging.

Characterization of the zero-force sensor conformation. FRET efficiency was measured using equation (1)

$$E = \left(1 - \frac{I_{DA}}{I_D}\right)\frac{1}{f_A} \quad (1)$$

where I_{DA} refers to the intensity of the EGF-PEG_x–Alexa Fluor 647 surface containing quench labeled streptavidin, I_D is the intensity of the EGF-PEG_x–Alexa Fluor 647 surface with unlabeled streptavidin and f_A is the labeling ratio of the acceptor[22]. These values were obtained by averaging the fluorescence intensity measured in five different areas for each substrate. The reported values are the average of three independent experiments. The calculated efficiency for each surface was then used to determine the average distance between fluorophore and quencher by,

$$E = \frac{1}{1 + \left(\frac{r}{R_0}\right)^6} \quad (2)$$

where R_0 is the Förster distance of the dye pair (6.9 nm according to the manufacturer) and r is the average distance between the fluorophores[22]. The predicted value for r was determined by adding the PEG Flory radius to the radii of the proteins that comprise the force sensor. The protein radius for EGF was estimated at 1 nm based on its crystal structure (Protein Data Bank (PDB): 2KV4), and for streptavidin the radius was estimated at 2 nm based on the crystal structure (PDB: 1SWB). The predicted r value was then compared to the FRET measured r value and reported in **Supplementary Figure 2**.

Fluorescence microscopy. Live cells were imaged in serum-free RPMI 1640 (Mediatech) medium formulated as described in the cell culture section at 37 °C, and fixed cells were imaged in 1% BSA in 1× PBS at room temperature. During imaging, physiological temperature was maintained with a warming apparatus consisting of a sample warmer and an objective warmer (Warner Instruments 641674D and 640375). The microscope used was an Eclipse Ti driven by the Elements software package (Nikon). The microscope features an Evolve electron multiplying charge-coupled device (CCD; Photometrics), an Intensilight epifluorescence source (Nikon) a CFI Apo 100× (numerical aperture (NA) 1.49) objective (Nikon) and a TIRF launcher with two laser lines: 488 nm (10 mW) and 640 nm (20 mW). This microscope also includes the Nikon Perfect Focus System, an interferometry-based focus lock that allowed the capture of multipoint and time-lapse images without loss of focus. The microscope was equipped with the following Chroma filter cubes: TIRF 488, TIRF 640, Cy5 and reflection interference contrast microscopy (RICM).

Image analysis. Images from sensor experiments were processed (using a custom macro in ImageJ (US National Institutes of Health)) from a single multipoint image file into individual tiff stacks containing each imaging channel. Separate macros were then used to isolate and background subtract the Alexa Fluor 647 EGF force channel. For all images, the LUT was linear and represented the full range of data as indicated by the calibration bar accompanying each image set. Analysis of images was performed with ImageJ and Nikon Elements software packages. ND2 image processing was done with several custom imageJ macros in combination with the LOCI bio-formats ImageJ plugin as well as the Nikon Elements software package. Sensor spot duration analysis was performed manually with the assistance of the SpotTracker 2D (ref. 23) and Multi Measure ImageJ plugins.

Quantitative force maps. To determine the absolute magnitude of forces detected by the sensor, a series of image operations were performed. First, the quenching efficiency image map was derived from the background subtracted TIRF 640 sensor signal image by using equation (3)

$$C = 1 - \frac{A}{B} \quad (3)$$

where A is the background-subtracted TIRF 640 sensor signal image, B is the average background-subtracted TIRF 640 image of a donor-only force probe obtained from a sample lacking the quencher and C is the resulting image which is a map of the quenching efficiency. Next, an image mapping the distance between the fluorophore and quencher was obtained by rearranging the FRET relation and applying equation (4)

$$D = R_0\left(\frac{1}{C} - 1\right)^{1/6} \quad (4)$$

where R_0 is the Förster radius of the quencher-fluorophore pair, and D is the resulting distance map[22]**.** This fluorophore-quencher distance image was then used to correct for the TIRF excitation intensity because the evanescent field intensity drops off exponentially in the z axis dimension. The penetration depth of the TIRF evanescent field was determined by equation (5)

$$d = \frac{\lambda}{4\pi\sqrt{n_2^2 \sin^2\theta - n_1^2}} \quad (5)$$

where d is the penetration depth of the evanescent field, n_2 is the index of refraction of glass (1.51), n_1 is the index of refraction

doi:10.1038/nmeth.1747

of water (1.33), λ is the wavelength (640 nm) and θ is the incident angle of the laser (~65°)[22]. The penetration depth can then be used along with the distance map to determine the corrected TIRF excitation intensity at each pixel. This is accomplished by applying equation (6)

$$S = Be^{-D/d} \tag{6}$$

where S is the scalar correction image, B is the donor only averaged image, D is the distance map image and d is the penetration depth of the evanescent field. The product of multiplying S by B gives the illumination intensity corrected distance map, E. To determine the average PEG resting conformation, the dimensions of EGF and streptavidin were subtracted from the corrected distance map, E. To calculate the extension of PEG from this resting state, the PEG resting state conformation was subtracted from the entire image. Finally, a quantitative force map was inferred by applying the extended WLC model to the distance map. The extended WLC approximation is made by applying equation (7) to image E

$$F = \frac{k_B T}{L_p}\left(\frac{E}{L} + \frac{1}{4\left(1-\frac{E}{L}\right)^2} - \frac{1}{4} + \sum_{i=2}^{i=7}\alpha_i\left(\frac{E}{L}\right)^i\right) \tag{7}$$

where F is the resulting quantitative force map image, k_B is the Boltzman constant, T is the temperature, L_p is the persistence length of PEG (0.38 nm), E is the corrected distance map and L is the end-to-end length of PEG_{24} (8.4 nm)[16].

Determination of EGFR phosphorylation and activation. HCC1143 cells were seeded onto the biosensor surfaces displaying EGF and incubated on the substrates for 30 min at 37 °C. Following initial imaging, the cells were fixed with 4% paraformaldehyde (Sigma) in 1× PBS and permeabilized with 0.1% Triton X (Sigma) in 1× PBS. Cells were then blocked overnight in 1% BSA at 4 °C. The next day, cells were incubated with a primary antibody to EGFR-pTyr1068 (Cell Signaling Technologies 3777s) at 1:200 dilution for 1 h at room temperature. The primary antibody was then washed out with 1× PBS and the cells were incubated with Alexa Fluor 488–labeled rabbit IgG secondary antibody (Invitrogen) at 1:1,000 dilution for 45 min. The secondary antibody was then rinsed out with 1× PBS, and the sample was imaged in TIRF mode at 488 nm as well as in the Alexa Fluor 647, brightfield and RICM channels using an epifluorescence source.

Actin inhibition. HCC1143 cells were serum-starved for ~18 h and split into two aliquots, one of which was treated with 4 µm latrunculin B (Sigma) for 30 min in DMSO (EMD Chemicals), and the other was treated with an equivalent amount of DMSO. Each aliquot was then plated onto an EGF-functionalized biosensor surface and incubated for 30 min at 37 °C. Cells were then imaged in the Alexa Fluor 647, brightfield and RICM channels.

CLC-eGFP transfection. HCC1143 cells were seeded on a 24-well plate in antibiotic-free media at a density of ~300,000 cells per well overnight. The cells were then transfected with the CLC-eGFP construct using Lipofectamine 2000 (Invitrogen) and following standard transfection protocols. These cells were then serum-starved overnight and used for experiments as indicated within 24 h of the transfection.

19. Clack, N.G., Salaita, K. & Groves, J.T. *Nat. Biotechnol.* **26**, 825–830 (2008).
20. Nair, P.M., Salaita, K., Petit, R.S. & Groves, J.T. *Nat. Protoc.* **6**, 523–539 (2011).
21. Galush, W.J., Nye, J.A. & Groves, J.T. *Biophys. J.* **95**, 2512–2519 (2008).
22. Lakowicz, J.R. *Principles of Fluorescence Spectroscopy*, 3rd edn. (Springer, New York, 2006).
23. Sage, D., Neumann, F.R., Hediger, F., Gasser, S.M. & Unser, M. *IEEE Trans. Image Process.* **14**, 1372–1383 (2005).